

Retrospective Model-Based Reduction of Low Spatial Frequency Intensity Variations in MR Images

William T. Katz, Ph.D., M.D.[†]
Neal F. Kassell, M.D.[†]
James R. Brookeman, Ph.D.[‡]

[†] Department of Neurosurgery
University of Virginia
Charlottesville, VA

[‡] Department of Radiology
University of Virginia
Charlottesville, VA

Please send correspondence:

William T Katz
www.billkatz.com

ABSTRACT

Operations using image intensities often assume the substances have spatially invariant intensities. This assumption may be incorrect in magnetic resonance imaging due to the low spatial frequency intensity variations introduced by the radio frequency coil and the image pulse sequence response. This paper describes a method for the indirect calculation of the sensitivity profile which uses the imaged brain as a qualitative phantom. The algorithm estimates ideal image intensities for likely brain voxels in a subsampled fashion, calculates an averaged sensitivity profile at each point in the subsampled grid, and then fits an order two three-dimensional polynomial to the averaged sensitivities. Since a voxel-based anatomic model is used to select the brain data points, user interaction is reduced to the initial registration of the image to Talairach space.

Key Words: Retrospective gradient removal, Model-based method, Three-Dimensional imaging, Talairach registration.

Introduction

With advances in medical imaging, three-dimensional (3D) images of unprecedented resolution can now be acquired in clinically-acceptable times. The large amount of image data, however, necessitates the use of a computer to automate to some degree the quantification and visualization of the data. When using computer-based processing, we would like the input 3D images to have sharply delineated intensity ranges for each tissue type. However, artifacts inherent in the imaging modality may introduce gradients, i.e. low spatial frequency intensity variations, within the images. While the human visual system perceives structures regardless of intensity drop-offs, practically all computational methods (such as simple thresholding) assume that homogeneous substances have spatially invariant intensities.

The problem of gradients in MR images has been studied by a number of researchers since the mid-1980's, and two assumptions are commonly made:

1) The observed intensity $I_{\text{obs}}(\vec{p})$ at a volume element (voxel) position \vec{p} is a product of the RF signals generated by the precessing protons, $I_{\text{true}}(\vec{p})$, and the sensitivity profile $S(\vec{p})$ of the RF coil and image pulse sequence response function used to generate the image:

$$I_{\text{obs}}(\vec{p}) = S(\vec{p}) \cdot I_{\text{true}}(\vec{p}) \quad (1)$$

2) The sensitivity profile $S(\vec{p})$ varies slowly relative to the higher spatial frequency components of anatomical object borders.

One approach uses a digital highpass filter [1] to selectively attenuate the low-frequency components corresponding to the gradient. While highpass filtering can suppress a low-frequency gradient, it unfortunately increases the intensities close to object surfaces - another artifact which blurs the intensity ranges for each tissue type.

A number of approaches estimate the sensitivity profile $S(\vec{p})$ and then divide the observed image with this estimated profile so $I_{\text{true}}(\vec{p}) = I_{\text{obs}}(\vec{p})/S(\vec{p})$. Hasselgrove and Prammer [2] suggested $S(\vec{p})$ be measured empirically by imaging a homogeneous phantom. Since the coil profile can vary over time and loading, "divide-by-phantom" approaches require phantom

imaging under conditions similar to those present during input image acquisition. Therefore, the correction of images cannot be performed retrospectively and the coil sensitivity of a head image cannot be modelled perfectly by a phantom differing in composition from the head.

Other approaches estimate $S(\vec{p})$ by performing a lowpass filtering operation using averaging or median filtering in the spatial domain [3, 4, 5]. Dividing $I_{\text{obs}}(\vec{p})$ by its low frequency version is mathematically equivalent to homomorphic filtering. Like highpass filtering, the main drawback of these techniques is the enhancement of intensities close to object surfaces. A number of researchers have addressed this problem and attempted to minimize large intensity changes along the edges. Adams [3] attempts to minimize the intensity drops in foreground/background transition areas by enforcing a minimum intensity before median filtering. Lim and Pfefferbaum [5] take a different approach and extend the brain intensities radially beyond the sharp brain-skull interface before applying an averaging filter. More recently, Harris et al. [6] minimize the effect of high-contrast edges by first segmenting brain and CSF areas and then setting background and CSF pixels to the mean intensity of the brain. While alleviating the more severe artifacts, none of the methods totally prevents intensity enhancement of structure boundaries relative to more homogeneous interior areas.

In addition to assuming a low spatial frequency gradient, we can model $S(\vec{p})$ as a function of limited order which adds some global constraints to how the sensitivity varies in space. A recent paper by Dawant et al. [7] models a 2D (slice) profile using thin plate splines. In their method, data points from a single substance (e.g. white matter) are selected interactively and the thin plate spline is fit either directly to the points or indirectly, through least-squares approximation, to a larger number of preclassified points. In contrast to the Dawant method, Tincher et al. [8] extended the “divide-by-phantom” approach by using a least-squares formulation to model 3D phantom data as a maximum variation order two polynomial. While both methods were successful in reducing the variation in homogeneous substance intensities, they suffer from requiring either excessive user interaction or a registered phantom image.

In this paper, we build on the modelling approaches using the *a priori* knowledge provided

by a registered voxel-based anatomic model and *treat the imaged brain as our phantom*. Rather than estimating $S(\vec{p})$ by using a phantom, lowpassed image, or user-defined points, we estimate $I_{\text{true}}(\vec{p})$ for likely brain voxels in a subsampled fashion, calculate an averaged sensitivity profile at each point in the subsampled grid, and then fit an order two, three-dimensional polynomial to the averaged sensitivities. Since a voxel-based model is used to select the data points, user interaction is reduced to the initial registration of the subject image to Talairach space.

Methods

Use of a Voxel-Based Anatomic Model

A subject's head image may be registered with a generic anatomic model by use of a proportional grid system; a useful method was proposed by Talairach [9] for stereotactic neurosurgery. Let \mathbb{N} be the set of natural numbers, $\vec{p} = [x \ y \ z]^T$ be a vector within \mathbb{N}^3 denoting a voxel's position in a 3D image with $0 \leq x \leq x_{\text{max}}, 0 \leq y \leq y_{\text{max}}, 0 \leq z \leq z_{\text{max}}$, and $G = \{0, 1, \dots, g-1\}$ be a set of positive integers representing the possible image values. Then the image intensity function can be defined as a mapping $I: \mathbb{N} \times \mathbb{N} \times \mathbb{N} \rightarrow G$ with the intensity of a voxel denoted as $I(\vec{p})$. Using the Talairach proportional grid system, we can register a head image and anatomic model to Talairach space and find a mapping $T: \mathbb{N} \times \mathbb{N} \times \mathbb{N} \rightarrow \mathbb{N} \times \mathbb{N} \times \mathbb{N}$ such that $T(\vec{p}) = \vec{v}$ when voxels of positions \vec{p} and \vec{v} within different images represent corresponding structures. The transformation T from one 3D image to another requires translation, rotation, and then a piecewise linear scaling within each of twelve regions of the Talairach proportional grid. This technique provides us with a powerful tool for employing *a priori* knowledge to our specific input image. While a number of models can be constructed for segmentation and classification of images [10], we limit the current discussion to the brain class model required for gradient reduction.

Although we do not have *a priori* knowledge of the range of intensities within a particular image, we do have *a priori* knowledge of the general distribution of gray and white matter within the brain. The brain class model M_{bc} attempts to capture unambiguous areas of white and gray

matter within the brain by combining the labelled images of n normal subjects. Given a finite set of labels $L_{BC} = \{\text{GrayMatter}, \text{WhiteMatter}, \text{NonBrain}, \text{Ambiguous}\}$, a labelled image has a mapping $\lambda_{BC}: \mathbb{N} \times \mathbb{N} \times \mathbb{N} \rightarrow L_{BC}$ where $\lambda_{BC}(\vec{p})$ gives the label for any voxel at position \vec{p} . The brain class model is then defined as

$$M_{bc}(\vec{p}) = \begin{cases} \Omega & \text{if } \lambda_{BC}^i(\vec{p}) = \Omega, \forall i = 1 \dots n \\ \text{Ambiguous} & \text{otherwise} \end{cases} \quad (2)$$

where $\lambda_{BC}^i(\vec{p})$ is the label at voxel \vec{p} in the subject image i . In other words, the brain class model records the labels attached to those voxels which were labelled identically across all n subject images. As currently implemented, the brain class model is constructed using three ($n = 3$) male volunteers aged 25 to 41.

Presumptive Class Histograms

A histogram is a convenient structure for analyzing and displaying the intensity distribution of a set of voxels. For each intensity x we find the set of voxels $V_x = \{\vec{p} \mid I(\vec{p}) = x\}$ and the histogram $h(x)$ gives the number of elements in the set V_x . If we use an entire image to determine the set V_x , it is very difficult to delineate the peaks corresponding to different substances. More selective histograms can be made by restricting the voxels used in histogram construction to those with high probability of being in a particular class according to our model. If the model is adequate, these presumptive class histograms will greatly emphasize individual class peaks compared to an indiscriminate histogram of the entire image. Two presumptive class histograms, necessary for the gradient reduction method, describe the intensity distribution of gray matter $h_{gm}(x)$ and white matter $h_{wm}(x)$ using the brain class model:

$$h_{gm}(x) = \sum_{\forall \vec{p} \in V_x} \delta(M_{bc}(\vec{p}), \text{GrayMatter}) \quad (3)$$

$$h_{wm}(x) = \sum_{\forall \vec{p} \in V_x} \delta(M_{bc}(\vec{p}), \text{WhiteMatter}) \quad (4)$$

where $M_{bc}(\vec{p})$ is given in Eq. (2) and the function δ tests the equivalence of two labels as in

$$\delta(\Psi, \Omega) = \begin{cases} 1 & \text{if } \Psi = \Omega \\ 0 & \text{if } \Psi \neq \Omega \end{cases} \quad (5)$$

We can model each presumptive class histogram as a mixture of gaussians using the Levenberg-Marquardt nonlinear fitting method [11]. The fitting procedure determines the mean of gaussians μ_{wm} and μ_{bm} for white and gray matter intensity distributions, respectively.

Estimation of the Sensitivity Profile

Estimation of I_{true} begins by partitioning the input 3D image to deal with subvolumes instead of individual voxels. Given a sampling rate κ , a voxel position \vec{p} , and a subsample vector $\vec{v} = \kappa \cdot \vec{p} \in \mathfrak{R}^3$, we define a mapping $s: \vec{p} \rightarrow \vec{q}$ where $\vec{q} \in \mathfrak{N}^3$ is the closest natural number approximation to \vec{v} . The function $s(\vec{p}) = \vec{q}$ gives the subvolume \vec{q} associated with any voxel \vec{p} .

Using the brain class model $M_{\text{bc}}(\vec{p})$ in Eq. (2), we can calculate the average observed intensities of likely brain voxels within each subvolume. The set of likely brain voxels V_B is the intersection of a set of ‘‘foreground’’ voxels and the set of voxels labelled as brain by the registered brain class model, i.e. those voxels \vec{p} where $M_{\text{bc}}(\vec{p}) = \text{GrayMatter} \vee \text{WhiteMatter}$. The set of foreground voxels can be determined by a number of methods (e.g. simple thresholding, k-means classification, etc.); the results given use a threshold determined by the gaussians fit to CSF, white matter, and gray matter presumptive histograms [10].

Each subvolume \vec{q} has some number of voxels n_q which are members of the set of likely brain voxels V_B . We calculate the following for each subvolume \vec{q} only if $n_q > 0$:

$$\hat{I}_{\text{obs}}(\vec{q}) = \sum_{\forall \vec{p} \mid s(\vec{p}) = \vec{q}} I(\vec{p}) / n_q \quad (6)$$

where $\hat{I}_{\text{obs}}(\vec{q})$ is the average of the observed intensities within a subvolume. We can also estimate $I_{\text{true}}(\vec{p})$ for likely brain voxels using

$$\hat{I}_{\text{true}}(\vec{q}) = \sum_{\forall \vec{p} \mid s(\vec{p}) = \vec{q}} I_{\text{est}}(\vec{p}) / n_q \quad (7)$$

where $\hat{I}_{\text{true}}(\vec{q})$ is the average of the expected intensities for a subvolume \vec{q} , and

$$I_{\text{est}}(\vec{p}) = \begin{cases} \mu_{\text{gm}} & \text{if } M_{\text{bc}}(\vec{p}) = \text{GrayMatter} \\ \mu_{\text{wm}} & \text{if } M_{\text{bc}}(\vec{p}) = \text{WhiteMatter} \end{cases} . \quad (8)$$

By substituting Eq. (6) and (7) in Eq. (1), we arrive at a computable form of the sensitivity profile for any subvolume \vec{q} with $n_q > 0$:

$$\hat{S}(\vec{q}) = \frac{\hat{I}_{\text{obs}}(\vec{q})}{\hat{I}_{\text{true}}(\vec{q})} . \quad (9)$$

We can then fit a second-order three-dimensional polynomial $\gamma(\vec{q})$ to $\hat{S}(\vec{q})$ using singular value decomposition to find the best least-squares approximation [8, 11]. Since our fit polynomial $\gamma(\vec{q})$ describes a continuous surface, we can compute the corrected intensity at any voxel \vec{p} of the image as $I_{\text{true}}(\vec{p}) \approx I(\vec{p}) / \gamma(\kappa \cdot \vec{p})$.

Results

The result of model-based gradient reduction on an image with a large intensity gradient is shown in Figure 1. Over a dozen data sets from different subjects have been processed with the technique as part of a segmentation pipeline [10]. In all cases, noticeable gradient effects were judged to be reduced through visual examination of pre- and post-processing pictures. While numerous case examples of improved segmentation are possible, we can evaluate retrospective model-based gradient reduction in isolation from the other stages of segmentation. The intent of gradient removal is to make a given tissue’s signature more homogeneous, less spatially variant. The effectiveness of the algorithm, then, can be directly tested using its objective as a criterion.

In the “divide-by-phantom” approach, a phantom of homogeneous composition is imaged and then used to correct subsequent imaging of the head. To evaluate retrospective gradient reduction, we can perform this process *in reverse*, using the image of the head to correct a phantom. First, an image of a subject’s head is obtained and immediately afterwards, we image a spherical phantom composed of copper sulfate solution without changing any significant imaging parameters (e.g. field-of-view, center line, etc). Voxels from the same location in the two images

(head and phantom) should correspond to the same volume element within the RF coil. Second, the sensitivity profile is modelled using the head image. This profile is used to correct the phantom image which is easily decomposed into foreground (copper sulfate solution) and background. Ideally, the corrected phantom should have all foreground voxels at one intensity. The effectiveness of gradient removal is quantitatively measured by the reduction of foreground intensity variance within the phantom image (Figure 2 and Figure 3).

Because variance is affected by scaling of the DC (zero spatial frequency) component, a normalization should be used so that the mean of the foreground is identical with and without gradient removal. A reasonable metric is the coefficient of variation (cv) defined as $cv = \sigma/\mu$. Retrospective model-based gradient removal reduced phantom foreground cv by 18.4% from 0.230 to 0.188. Over the phantom area covered by the brain, however, foreground cv was reduced by 27.2% from 0.215 to 0.156. Since the sensitivity profile is modelled using a limited area (i.e. the brain), significant inhomogeneities outside the brain may not be removed unless extrapolation of the profile coincides with the real sensitivity at those locations. The brain area, however, comprises the “sweet spot” of the model-based gradient removal.

The F-ratio test can also be used to determine if the corrected and uncorrected foreground variances are statistically significant. In order to reduce the correlation between the samples, 1001 randomly distributed points within the phantom foreground were selected. The intensities were normalized so that the means of the corrected and uncorrected data sets were identical. The test statistic was calculated as

$$F = \frac{\sigma_{\text{uncorrected}}^2}{\sigma_{\text{corrected}}^2} = \frac{114678.5}{73254.1} = 1.57 \quad (10)$$

where the null hypothesis $H_0: \sigma_{\text{uncorrected}}^2 = \sigma_{\text{corrected}}^2$ is rejected if F deviates to strongly from unity. In this particular case, with 1000 degrees of freedom (from the 1001 sample points), the alternate hypothesis $H_A: \sigma_{\text{uncorrected}}^2 > \sigma_{\text{corrected}}^2$ is accepted with a greater than 99% level of significance since

$$\begin{aligned}
 F &\gg F_{0.01, 1000, 1000} \approx 1.159 \\
 \therefore p(H_0) &\ll 0.01
 \end{aligned}
 \tag{11}$$

From Eq. (11), we can say with some certainty that retrospective model-based gradient removal significantly decreased the variance of the phantom image.

The phantom data also allows us to quantitatively assess the impact of image partitioning on gradient removal. As described earlier, the input 3D image is divided into subvolumes using the parameter κ . Larger values of κ correspond to finer subdivision whereas smaller values of κ correspond to increased subvolume size (and hence averaging of the constituent voxels). The coefficient of variation cv was determined after varying κ (1/8, 1/4, and 1/2) and in all cases, the cv of the entire foreground and the foreground areas corresponding to brain were reduced by using the model-based gradient removal method. Setting κ to 1/8, 1/4, and 1/2 resulted in a brain area foreground cv of 0.173, 0.162, and 0.157, respectively. In general, increased κ gives better results at the (negligible) cost of added time and memory requirements for fitting on a larger data set. Using a Hewlett-Packard 9000/735 workstation with 150 MB memory, the model-based gradient reduction algorithm (including user-specified Talairach registration) requires less than five minutes.

Discussion

While a phantom study in many respects is a “gold-standard,” the effects of loading on the RF coil may change the sensitivity profile between a head image and the phantom image. Partly to avoid such complications, recent papers by other researchers have suggested employing user-defined sets of points to describe the intensity distribution of substances. This paper describes a method for employing voxel-based anatomic models which allows construction of presumptive class histograms and automation of coil sensitivity estimation.

The proposed method has two advantages. First is the ability to perform retrospective analysis of images. Second is the limiting of user interaction to a simple image registration

procedure requiring only the marking of a few landmarks. The method has been shown to reduce the variation of intensities among over a dozen head images as well as within a spherical test phantom.

An interesting byproduct of the polynomial modelling is the robustness of the model-based gradient reduction method with respect to brain loss. It is reasonable to assume that commercial RF coils used in MRI are symmetrical about their center. With this property in mind, we can see how a second-order polynomial, with its lack of multiple inflection points, might easily reflect the symmetry of coil sensitivity about a center.

Because only foreground voxels are used as data points for polynomial fitting, absence of brain matter results in removal of points from the data set. If the brain is centered within the RF coil, removal of brain matter in one cerebral hemisphere - with the accompanying loss of data for sensitivity fitting - can be compensated by the symmetrical sensitivity information found in the other hemisphere. This property, in part, makes the model-based gradient removal method extremely robust with respect to loss of brain tissue. Tests of method robustness have been performed by removing a very large part of the brain image, as in the case of a total hemispherectomy. Despite the loss of many data points, the data from undestroyed points in symmetric parts of the sensitivity profile permitted the fitting procedure to produce a qualitatively similar polynomial to one constructed using the undecimated image.

In conclusion, use of the *a priori* knowledge provided by registered voxel-based anatomic models can allow fast semi-automatic reduction of low spatial frequency intensity variations in a robust retrospective manner.

Acknowledgements

The authors would like to thank Jim Bertolina for his help in providing the images for this study. The work has been partially supported by the Medical Scientist Training Program, University of Virginia.

References

- 1 Sharples T, Lufkin R, Hanaffee W. Dynamic range compression in surface coil MRI. *Magn Reson Med* 1986; **4**: 165.
- 2 Haselgrove J, Prammer M. An Algorithm for Compensation of Surface-Coil Images for Sensitivity of the Surface Coil. *Magn Reson Med* 1986; **4**: 469-472.
- 3 Adams AH. "Digital picture processing and pattern recognition as applied to Magnetic Resonance images of diseased human breast tissue," Ph.D. dissertation, University of Virginia, 1989.
- 4 Brey WW, Narayana PA. Correction for intensity falloff in surface coil magnetic resonance imaging. *Med. Phys.* 1988; **15**: 241-245.
- 5 Lim KO, Pfefferbaum A. Segmentation of MR Brain Images into Cerebrospinal Fluid Spaces, White and Gray Matter. *J Comput Assist Tomogr* 1989; **13**: 588-593.
- 6 Harris GJ et al. MR Volume Segmentation of Gray Matter and White Matter Using Manual Thresholding: Dependence on Image Brightness. *AJNR* 1994; **15**: 225-230.
- 7 Dawant BM, Zijdenbos AP, Margolin RA. Correction of Intensity Variations in MR Images for Computer-Aided Tissue Classification. *IEEE Trans Med Imaging* 1993; **12**(4): 770-781.
- 8 Tincher M, Meyer CR, Gupta R, Williams DM. Polynomial Modeling and Reduction of RF Body Coil Spatial Inhomogeneity in MRI. *IEEE Trans Med Imaging* 1993; **12**: 361-365.
- 9 Talairach J, Tournoux P. *Co-Planar Stereotaxic Atlas of the Human Brain*. New York: Georg Thieme Verlag, 1988.
- 10 Katz WT. "Semiautomated Segmentation and Display of Three-Dimensional Images of the Head," Ph.D. dissertation, University of Virginia, 1994.
- 11 Press WH, Teukolsky SA, Vetterling WT, Flannery BP. *Numerical Recipes in C*. Cambridge: Cambridge Univ. Press, 1992.

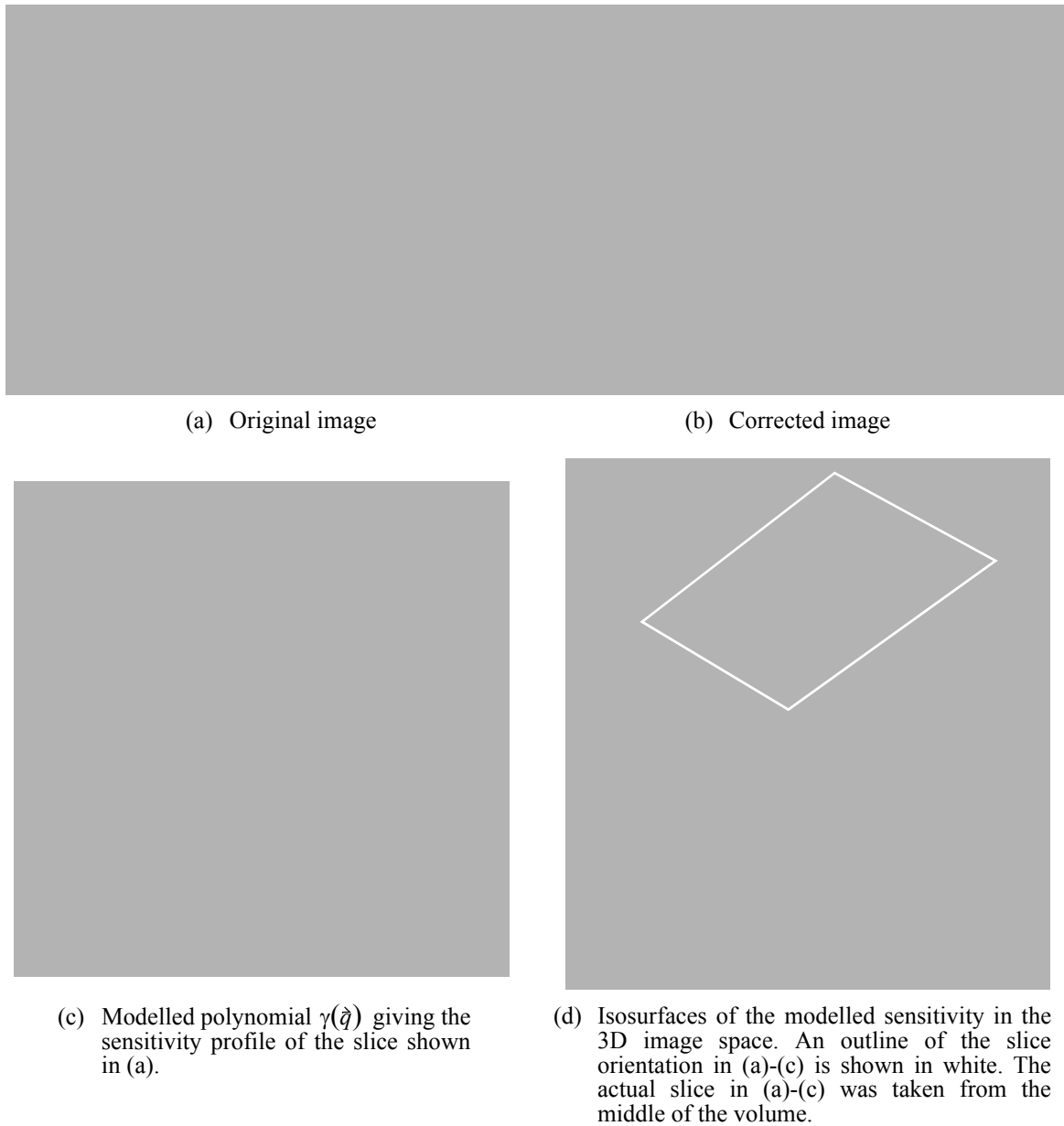


Figure 1. Sensitivity analysis of MR imaging using a knee coil.

Model-based gradient reduction was applied to a 3D MR image of a cadaver acquired with a knee coil. As seen in the isosurface figure (d), the sensitivity drops significantly as we moves away from the Helmholtz coils.

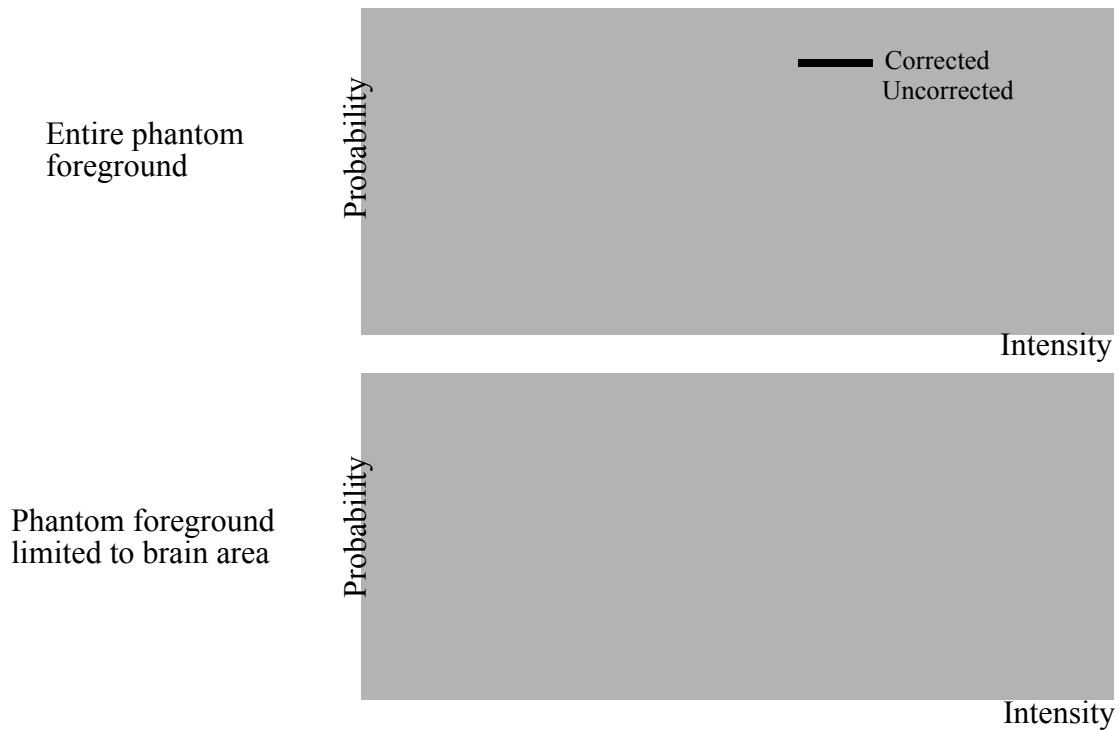


Figure 2. Phantom foreground histograms.

A sensitivity profile modelled from a head image was used to reduce the intensity variations in a phantom. Note the reduction in variance of the foreground mode after the phantom image was corrected by the model-based gradient removal method. Correction was more significant for the “sweet spot” area corresponding to the brain [bottom graph].

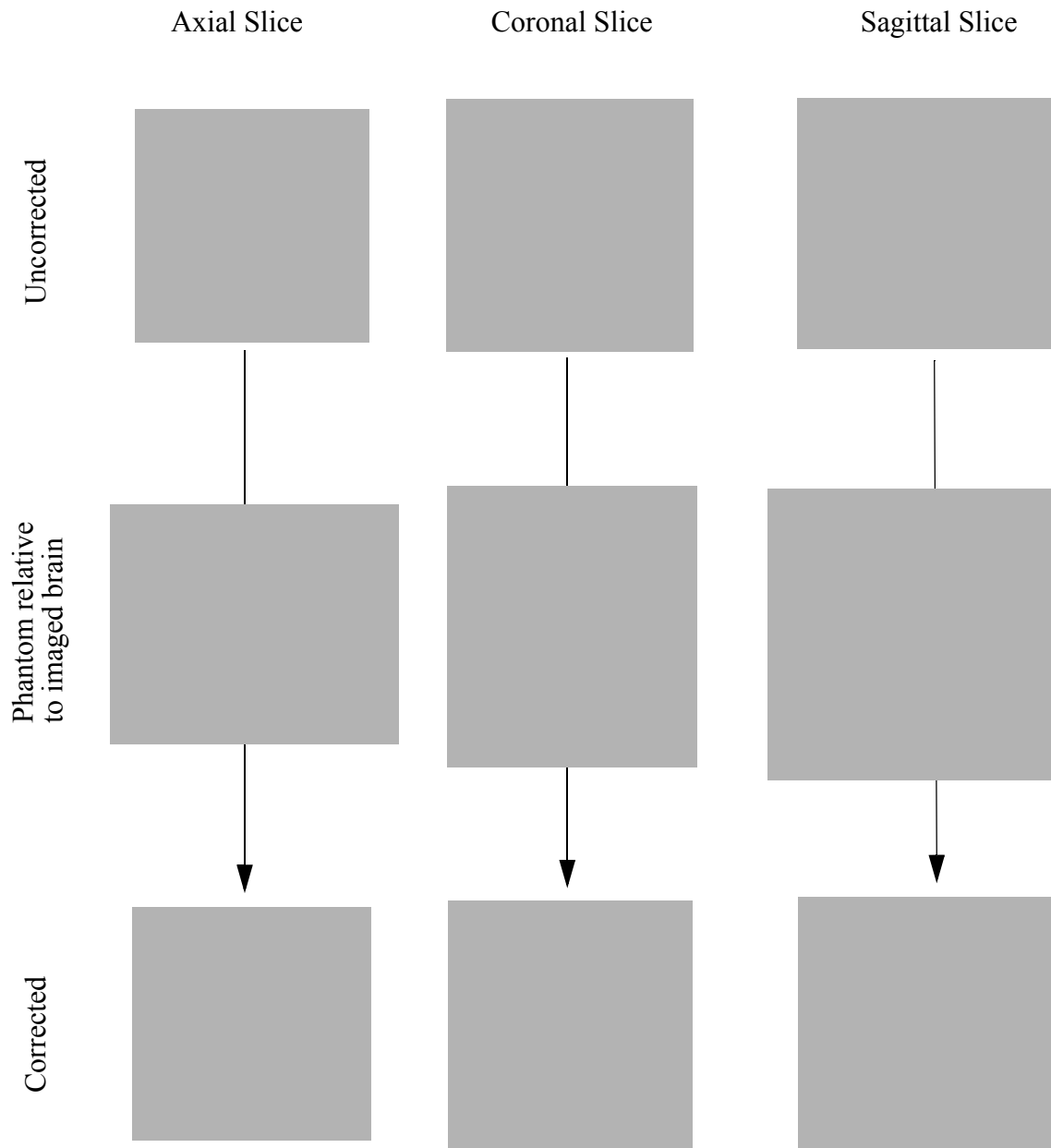


Figure 3. Correction of phantom using head image.

An image of a phantom (top row) was corrected using the sensitivity profile modelled from a head image (middle row, phantom position outlined in white). Phantom correction is least obvious in the axial slice (left column) where the actual head image shows little gradient. Gradient removal is most obvious along the superior-inferior axis; a result which undoubtedly follows from the significant image loss along the superior margin of the brain.